



TSF0010

## On characteristics of jet from two-dimensional nozzle with a lip

S. Ysasuda, R. Ogura, Y. Otomine and K. Hirata\*

Department of Mechanical Engineering, Doshisha University, Kyoto 610-0321, Japan

\* Corresponding Author: khirata@mail.doshisha.ac.jp

**Abstract.** In the present study, as well as our previous study (Hirata *et al.*, 2010), we research the jet from an asymmetrical two-dimensional nozzle, whose asymmetry is introduced by the effect of the lip length of the nozzle. Especially, we focus our attention to the influence of the lip length upon such a flow at a lower Reynolds number within much wider parameter's range than previous study. Experiments are conducted at a Reynolds number of 1,000. The aspect ratio of the nozzle exit is fixed to 300. And, the lip length is 0, 2.0*h*, 3.3*h*, 4.0*h*, 5.0*h*, 6.0*h*, 8.0*h* and 10*h*, where *h* denotes the height of the nozzle exit. As a result, we have shown turbulence-intensity profiles in addition to mean-velocity profiles at various downstream sections, in order to reveal fundamental characteristics of the jet. And, we have confirmed the effectivity of lip's control upon jet's deflection on the basis of both time-mean velocity and jet's turbulence even at a low Reynolds number.

### 1. Introduction

Mixing/diffusion enhancement is one of the key technologies in various environmental aspects, and has become needed in chemical reactors, heat exchangers, burners/combustors, air conditioners and so on. Jets are known to be useful for such mixing/diffusion enhancements (see Hirata *et al.* (2009) [1] and Funaki *et al.* (2009) [2]).

Most of past studies concern a circular jet, namely, the jet from a nozzle with a circular cross section. On the other hand, we have been recently focusing our interest upon non-circular jets, to achieve more efficient mixing/diffusion enhancements. Among such non-circular jets, a plane jet has fundamental and practical importance, as it is applicable for various fields such as (1) drying/cooling of plastic films and fabrics, (2) cleaning/draining/drying of manufacturing products, (3) flow controls inside burners and at furnace entrances and (4) efficient and smart air conditioning devices such as air curtains and air screens.

Now, we concentrate our notice upon turbulent and free plane jets at high Reynolds numbers  $Re$ 's, considering practical importance in many industrial fields. Thus far, there have been several researches concerning the turbulent and free plane jet (for example, see Förthmann (1936) [3], Goertler (1942) [4], Zijnen (1958) [5], Quinn (1992) [6], Mi *et al.* (2005) [6] and Deo (2005) [8]). However, most of them are about the jet emitted from a symmetrical nozzle, and there have been only a few researches concerning the jet emitted from an asymmetrical nozzle, such as Horne *et al.* (1981) [9], Husain & Hassain (1983) [10], Kiwata *et al.* (2009) [11] and Hirata *et al.* (2010) [12]. Our knowledge about such asymmetrical plane jets has not been enough yet, in spite of their potentials to various applications like (1) increase/decrease of the flow entrainment or the streamwise growth of flow rate, (2) promotion/suppression of the decay of flow velocity, (3) control of the jet's direction, (4)

realisation of oscillatory or pulsative jets, and (5) generation of the asymmetrical flow fields concerning time-mean velocity, turbulence and so on.

In the present study, as well as our previous study (Hirata et al. (2010)) [12] at a Reynolds number of 6,000, we research the turbulent and free-plane jet from an asymmetrical two-dimensional nozzle, whose asymmetry is introduced by the effect of the lip length of the nozzle. —Among various control methods to asymmetrise a plane jet, such as (1) asymmetrical nozzle geometry, (2) insertion of a downstream object or a nozzle-surface object and (3) addition of secondary jets, the lip-length control has advantages of both (1) simple geometry with less control parameters and (2) easier change of control-parameter values.— Especially, we focus our attention to the influence of the lip length upon flow-turbulence characteristics in addition to time-mean-flow ones at a lower Reynolds number within much wider parameter's range than the previous study. Experiments are conducted at a Reynolds number of 1,000. The aspect ratio of the nozzle exit is fixed to 300. And, the lip length  $l$  varies in a wide range of  $0 - 10.0h$ , where  $h$  denotes the height of the nozzle exit. Using a hot-wire anemometer, we measure mean-velocity and turbulence-intensity profiles at various downstream sections, in order to reveal fundamental characteristics of the jet in both the near and far downstreams.

## 2. Experimental Method

Figure 1 show the present model, namely, a plane jet issued into an open-space and stationary fluid from an asymmetrical two-dimensional nozzle with a different dimension  $l$  between both the ends of the upper and lower halves of a nozzle, which is hereinafter called as a “lip length.”

In the present study, the upper half of the nozzle is longer than the lower half by  $0 - 10h$ , where  $h$  ( $= 1.5 \times 10^{-3} \text{m}$ ) represents the height of the nozzle exit, which is used as a characteristic length scale. Hereinafter, the upper and lower sides of the nozzle are referred to as “lip side LS” and “no-lip side NLS,” respectively.

Figure 1 also shows the present coordinate system, together with important physical parameters. The coordinate's origin  $O$  is at the nozzle exit on the mid-plane and on the span-centre plane. Strictly speaking, “the nozzle exit” is at the end of the lower half of the nozzle. The coordinate system is a Cartesian and right-handed one with a streamwise component  $x$ , a cross-streamwise (span-wise) component  $y$  and another cross-streamwise (transverse) component  $z$ . The governing equations for this match are incompressible 3D Navier – Stokes equations, as the Mach number  $Ma$  is less than 0.03 at  $Re = 1,000$  and less than 0.2 at  $Re = 6,000$ .

We define the magnitude value  $u$  of flow velocity as  $|\mathbf{v}|$ . Both  $u_{\text{mean}}$  and  $u_{\text{rms}}$  are functions of  $x$  and  $z$  alone, where subscripts “mean” and “rms” denote time-mean and root-mean-square, respectively. The half width  $2b$  on the transverse velocity profile is defined as the width at whose boundaries  $u_{\text{mean}} = (u_{\text{mean}})_{\text{max}}/2$ , where a subscript “max” denotes the maximum value of  $u$  at each  $x$ .

As a geometric control parameter of the concerning jet, we consider a reduced lip length  $l/h$ . And, as a kinetic control parameter, we consider the Reynolds number  $Re$ . Its definition is as follows,  $Re \equiv U_{0 \text{ mean}} h / \nu$  where a characteristic velocity scale  $U_{0 \text{ mean}}$  denotes the time-mean velocity at the nozzle exit on the mid-plane and on the span-centre plane.

We define an aspect ratio  $AR$  of the nozzle exit by  $w/h$ , where  $w$  is the width of the nozzle exit. The nozzle has such a large aspect ratio  $AR$  ( $\equiv w/h$ ) as 300.

Table 1 summarises the values of main experimental parameters in dimensional and non-dimensional forms. The time-mean averaging is carried out over more than 20 sec, to ensure enough accuracy and reproducibility.

In the present experimental apparatus, working fluid is air. Air is driven by a blower. And, through an enough-long straight pipe with a constant cross-section area of 1.8m in length and 56mm in inner diameter, air is issued out of an asymmetrical two-dimensional nozzle into stationary open space with a fully-developed velocity profile. Using a hot-wire anemometer with an I-type probe whose temperature effect is compensated by a cold-wire probe, we measure  $u$  at many locations downward the nozzle exit. The insertion angle of the I-type probe is determined so as to minimise the disturbance by the probe.

### 3. Results and Discussion

#### 3.1. Mean-Velocity Profiles

In this and following sections 3.2 – 3.4, we consider streamwise distributions of such a quantity as  $u_{\text{mean}}$ , standing on the measurements by a hot-wire anemometer at various values of  $x/h$  and  $z/h$  on the span-centre plane.

Figure 2 shows a typical example of transverse profiles of  $u_{\text{mean}}$ . Specifically speaking, this figure is for  $l/h = 5.0$  at several values of  $x/h$ . At the nozzle exit (at  $x/h = 0$ ), a clear potential core of the jet exists at  $z/h = -0.5 - 0.5$ . However, there is not any data at  $z/h = 0.5 - 2.7$  in the profile at  $x/h = 0$ , due to the existence of the lip. Supplementarily speaking, very slow flow exists in a wide range of  $|z/h| > 2$ . Of course, we have confirmed that  $u_{\text{mean}}$  asymptotes to zero at  $z/h = \pm\infty$ . The slower flow is considered to be related with the entrainment of ambient fluid into the jet. As  $x/h$  increases from zero, the profile becomes gradual, that is, its peak becomes low and its foot becomes wide. As well as the profile at  $x/h = 0$ , the profiles at  $x/h \neq 0$  accompany the slower flow related with the entrainment. In addition, we can see that the profile centre tends to shift to the positive  $z/h$  direction with increasing  $x/h$ . This will be discussed in Fig. 5.

#### 3.2. Streamwise Decay of Maximum Mean-Velocity

Figure 3 shows the streamwise distributions of the maximum mean-velocity  $(u_{\text{mean}})_{\text{max}}$  for various values of  $l/h$ , in order to observe the streamwise variation of the jet. This figure also shows the theory by Tollmien (1945) [9] for two-dimensional free jet and the experiments by Mi et al. (2005) [6] for symmetrical nozzles and the experiments by Kiwata et al. (2009) [8] for asymmetrical nozzles.

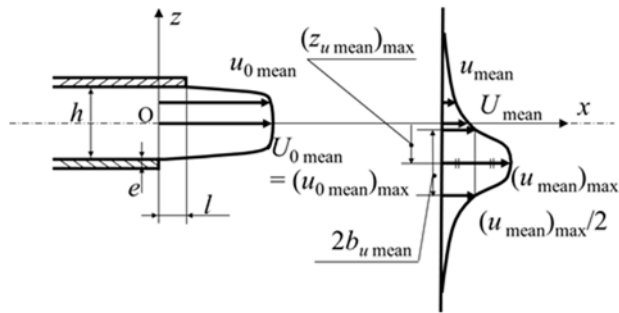
The present streamwise distributions are almost similar with the Tollmien's theory, and then with those at  $Re = 6,000$  [12]. To be district, all the results at each  $x/h$  are slightly less than the Tollmien's theory, being independent of the values of  $l/h$ . This is considered to be an influence of  $Re$ , if we remind the good agreement between experiments and the theory at  $Re = 6,000$  [12].

Next, we consider  $(u_{\text{mean}})_{\text{max}}$  in the near downstream. According to Rajaratnam (1976), [9] the potential core of a two-dimensional jet exists at  $x/h \leq 6$ . All the present results are consistent with this, being independent of the values of  $l/h$ . Because,  $(u_{\text{mean}})_{\text{max}}/U_{0 \text{ mean}}$  is approximately equal to unity at  $x/h \leq 10$ .

Finally, in figure 4, we show the streamwise distributions of  $(u_{\text{mean}})_{\text{max}}$  with the abscissa of  $x/D_e$  instead of  $x/h$ . We should note that both the abscissa and the ordinate have logarithmic scales..

According to Mi et al. (2005) [6], we see (1) the potential core zone, (2) quasi-plane-jet zone, (3) the transition zone and (4) quasi-axisymmetric-jet zone in sequence, as  $x/D_e$  increases. And, the larger  $AR$  is, the smaller the value of  $x/D_e$  where the quasi-plane-jet zone appears. Besides, the larger  $AR$  is, the wider the range of  $x/D_e$  for the quasi-plane-jet zone is. In the quasi-plane-jet zone and the quasi-axisymmetric-jet zone,  $(u_{\text{mean}})_{\text{max}}/U_{0 \text{ mean}}$  is in proportion to  $x^{-1/2}$  and  $x^{-1}$ , respectively.

All the present data at  $x/D_e \gtrsim 1$  collapse on a common straight line which is in proportion to  $x^{-1/2}$ . This suggests good two-dimensionality of the jet. In addition, we can confirm a consistency with Mi et al.; namely, the present value of  $(u_{\text{mean}})_{\text{max}}/U_{0 \text{ mean}}$  is always smaller than Mi et al. at each  $x/D_e$ . This is reasonable, if we remind such a high  $AR$  as 300, which is larger than Mi et al., being independent of the values of  $l/h$ . Complementarily speaking, it seems difficult to compare the above results with Kiwata et al. (2009), due to their different velocity profile caused by much different nozzle geometry with a far-upstream contraction.



$x$ : streamwise coordinate     $u_{0 \text{ mean}}$ : time-mean velocity at the nozzle exit  
 $h$ : height of a nozzle exit     $U_{\text{mean}} = u_{\text{mean}}$  on the midplane (at  $z = 0$ )  
 $l$ : lip length     $u_{\text{mean}}$ : flow velocity  
 $e$ : thickness of a nozzle     $2b_{u \text{ mean}}$ : half width  
 $(z_{u \text{ mean}})_{\text{max}}$ :  $z$  at  $u_{\text{mean}} = (u_{\text{mean}})_{\text{max}}$

**Figure 1.** Model and coordinate system.

**Table 1.** Experimental parameters.

$h$ (m)	$1.5 \times 10^{-3}$
$l$ (m)	$0.0, 3.0 \times 10^{-3}, 5.0 \times 10^{-3}, 6.0 \times 10^{-3}, 7.5 \times 10^{-3}, 9.0 \times 10^{-3}, 12 \times 10^{-3}$ and $15 \times 10^{-3}$
$w$ (m)	$450 \times 10^{-3}$
$U_0$ (m)	10
$l/h$	0, 2.0, 3.3, 4.0, 5.0, 6.0, 8.0 and 10
$AR (= w/h)$	300
$Re$	1,000
Sidewalls	No

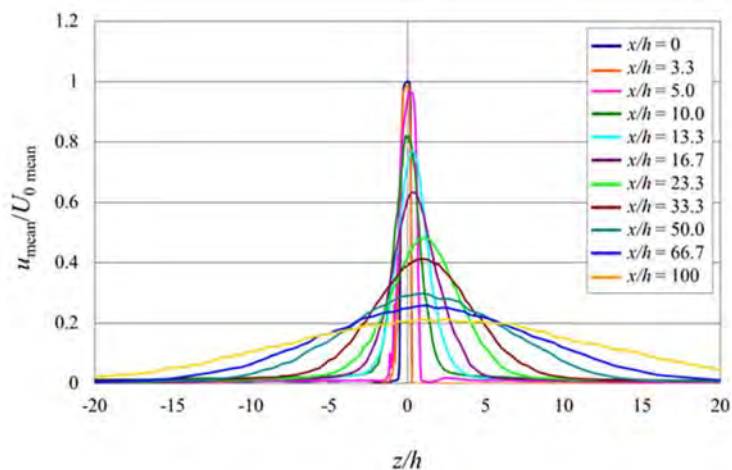


**Figure 2.** Mean-velocity profiles in the  $z$  direction at midspan ( $y/h = 0$ ) for  $l/h = 5.0$  and  $Re = 1,000$ .

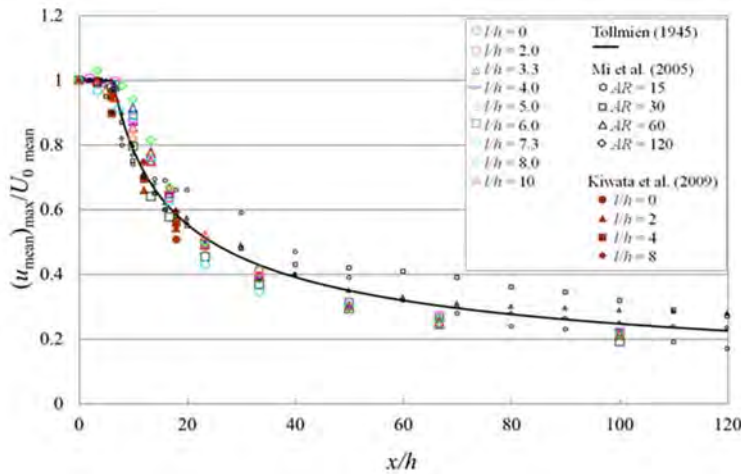


**Figure 3.** Streamwise distributions of the maximum mean-velocity at midspan ( $y/h = 0$ ) for  $l/h = 0 - 10$ ,  $Re = 1,000$ .

All the present data at  $x/D_e = 0.4 - 1$  collapse on another common straight line which is in proportions to  $x^{-0.8}$ . This is also considered to be another influence of  $Re$ , if we remind that all the data for  $Re = 6,000$  is in proportions to  $x^{-1/2}$  even at  $x/D_e = 0.3 - 1$  [12].

### 3.3. Streamwise Variation of Jet's Bias on Mean-Velocity

Figure 5 shows the streamwise distributions of a jet's bias  $(z_{u \text{ mean}})_{\text{max}}$  on mean-velocity, namely, a local mean-velocity-profile centre, for several values of  $l/h$ . We define  $(z_{u \text{ mean}})_{\text{max}}$  as the value of  $z$  where the transverse mean-velocity profile attains the maximum  $(u_{\text{mean}})_{\text{max}}$  at each  $x$ , as shown in figure 2. Error bars in figure 5 show the boundaries of the region where  $u_{\text{mean}} \geq 0.95 U_{0 \text{ mean}}$ . This region could be approximately regarded as the potential core.

At first, when we consider the far downstream at  $x/h \geq 10$ , we can clearly confirm the streamwise growth of the jet bias suggested in figure 2. Concretely speaking, the jet bias for  $l/h = 0$  is slightly negative and is almost in proportion to  $x/h$ . Namely, the jet direction is not horizontal, but somewhat downward. This is considered to be related with the incompleteness of the symmetry in nozzle's geometry, even for  $l/h = 0$ . In addition, the jet axis is almost linear.

As well, the jet biases for  $l/h = 2.0$  and  $3.3$  show the above two features such as (1) the downward deflection and (2) the spatial linearity of the jet axis. However, from a quantitative viewpoint, we can find an effect of  $l/h$  upon the jet bias, if we compare the results for  $l/h = 0$ . Namely, by the  $l/h$  effect, the large  $l/h$  becomes, the more downward the jet deflection is.

In contrast with the jet biases for  $l/h = 0, 2.0$  and  $3.3$ , the jet biases for  $l/h = 4.0$  and  $5.0$  indicate such a different feature as the jet deflection is upward.

Again, the jet biases for  $l/h = 6.0$  and  $8.0$  shown the same two features for  $l/h = 0$  as (1) the downward deflection and (2) the spatial linearity of the jet axis. From a quantitative view point, we can find an effect of  $l/h$  upon the jet bias. Namely, the jet's biases for  $l/h = 6.0$  and  $8.0$  almost coincide with that for  $l/h = 0$ . However, from a quantitative viewpoint, we can find a  $l/h$  effect upon the jet's bias. Namely, the jet's bias for  $l/h = 10$  almost coincide with those for  $l/h = 2.0$  and  $3.3$ .

As well, the jet's bias for  $l/h = 10$  shows the same two features for  $l/h = 0$ . Next, we consider the near downstream at  $x/h < 10$ , where figure 5 is not appropriate owing to condensed results at  $x/h < 10$ . To conclude, we can again confirm that the present results coincide with Rajaratnam (1976) [9], as the potential core of a two-dimensional jet exists at  $x/h \leq 10$  for all the tested  $l/h$ .

Incidentally speaking, concerning the shape of the potential core, it seems difficult to find out any clear  $l/h$  effects. Especially for  $l/h = 0$ , the upper and lower outer boundaries of the potential core are

fairly symmetrical concerning the horizontal axis  $(z_{u \text{ mean}})_{\text{max}}/h = 0$ . This suggests such a fact that the nozzle axis is accurately installed parallel to the horizontal axis, while the jet bias exists in the downstream even for  $l/h = 0$ .

### 3.4. Streamwise Growths of Half Width on Mean-Velocity and of Flow Rate

Figure 6 shows the streamwise distributions of the half width  $2b_{u \text{ mean}}$  on mean-velocity profile at midspan ( $y/h = 0$ ) for several values of  $l/h$ . Both the axes are normalised by  $h$ . For reference, the figure also shows the theory by Rajaratnam (1976) [9] such as

$$2b_{u \text{ mean}} = 0.20x. \quad (1)$$

At  $x/h \lesssim 10$ ,  $2b_{u \text{ mean}}/h$  is almost unity, being independent of  $l/h$ . This is consistent with the existence of the potential core. At  $x/h \gtrsim 10$ ,  $2b_{u \text{ mean}}/h$  increases linearly with increasing  $x/h$ . Moreover, we can see that all the results almost collapse on the theory by Rajaratnam for a two-dimensional free jet, being independent of  $l/h$ . To be strict, all the results are slightly larger than the Rajaratnam's

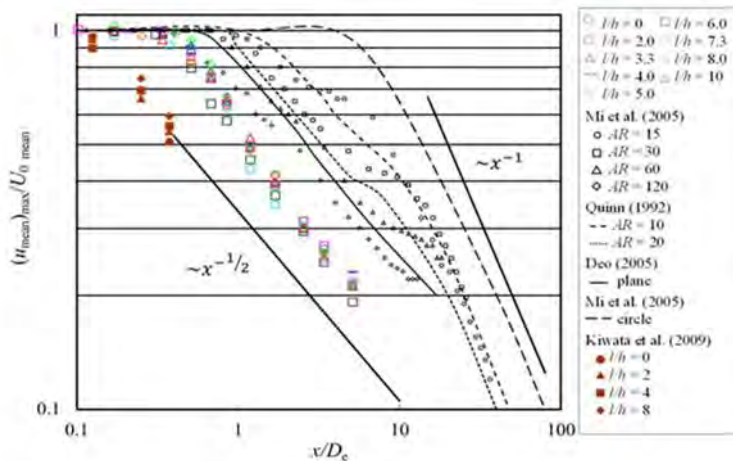


**Figure 4.** Streamwise distributions with logarithmic scales of the maximum mean-velocity at midspan ( $y/h = 0$ ), for  $AR = 300$ ,  $l/h = 0 - 10$  and  $Re = 1,000$ . The abscissa is normalised by an equivalent diameter  $D_e$ .

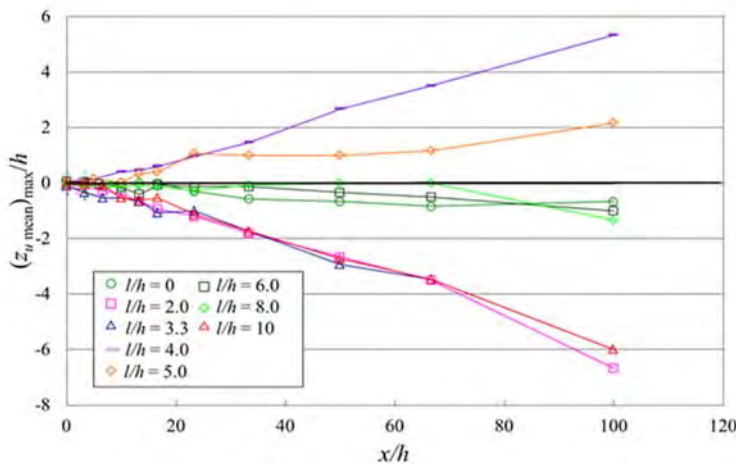


**Figure 5.** Streamwise distributions of jet's bias  $(z_{u \text{ mean}})_{\text{max}}$  of mean-velocity profile at midspan ( $y/h = 0$ ) for  $l/h = 0 - 10$  and  $Re = 1,000$ .

theory, as well as those for  $Re = 6,000$  [12].

Figure 7 shows the streamwise distribution of the local time-mean (volumetric) flow rate  $Q$  per unit span at midspan ( $y/h = 0$ ) for  $l/h = 0 - 10$ . The ordinate is normalised by  $Q_0$ , which denotes the flow rate from the nozzle exit. For reference, the figure also shows the theory by Albertson et al. (1950) [9] for a two-dimensional free jet such as

$$\frac{q}{Q} = 0.44 \sqrt{\frac{2x}{h}}, \quad (2)$$

and experiments by Kiwata et al. (2008) [8] for asymmetrical nozzles.

For all  $l/h$ 's,  $Q/Q_0$  monotonically tends to increase with increasing  $x/h$ . All the results for every  $l/h$ 's are always smaller than Albertson et al, being independent of  $x/h$ . This suggests that the flow entrainment can be suppressed not by the lip but by the influence of  $Re$ , if we remind the results at high  $Re$  where  $Q/Q_0$  always larger than Albertson et al [12].

To summarise the above, we can see a distinctive influence of  $l/h$  only concerning (1) the jet bias, but cannot see it concerning (2) the maximum mean-velocity, (3) the half width and (4) the time-mean local flow rate. In comparison with high  $Re$  [12], we can see four influences of  $Re$  concerning (1), (2) and (4), expect for (3). It seems difficult to directly explain the influence of  $Re$  concerning (1), although the two influences of  $Re$  concerning (2) and (4) seems consistent.

### 3.5. Turbulence-Intensity profiles

In this and following sections 3.6 – 3.8, we consider streamwise distributions of such a quantity as  $u_{rms}$ , standing on the measurements by a hot-wire anemometer at various values of  $x/h$  and  $z/h$  on the span-centre plane.

Figure 8 shows a typical example of transverse profiles of  $u_{rms}$ . Specifically speaking, this figure is for  $l/h = 3.3$  at several values of  $x/h$ . At the nozzle exit (at  $x/h = 0$ ), a sharp peak exists at  $z/h = -0.5$ , which corresponds to a shear layer on the potential-core boundary. At  $x/h = 3.3$ , another sharp peak exists at  $z/h = 0.5$ , where the peak value of  $u_{rms}/(u_{mean})_{max}$  is larger than that at  $z/h = -0.5$ . As  $x/h$  increases from 3.3, both the two peak values of  $u_{rms}/(u_{mean})_{max}$  and both the width between the peaks and the of foot of  $u_{rms}/(u_{mean})_{max}$  increase.

In addition, we can confirm both (1) the profile asymmetry and (2) the profile-centre bias. The former is represented by the difference between the two peak values of  $u_{rms}/(u_{mean})_{max}$ , and is quenched at such a large  $x/h$  as 100. Till the quench, the superiority in the value of  $u_{rms}/(u_{mean})_{max}$  usually switches between the two peaks (to be discussed in figure 9). The latter intensifies with increasing  $x/h$ , as well as the profile of  $u_{mean}/U_{0\ mean}$ . The above features are commonly seen for other values of  $l/h$ .

### 3.6. Streamwise Growth/Decay of Maximum Turbulence-Intensity

Figure 9 shows the streamwise distributions of the maximum turbulence-intensity  $(u_{rms})_{max}$  on lip and no-lip sides for  $l/h = 5.0$ , in order to observe the streamwise variation of the jet.

At  $x/h \gtrsim 10$ , we can see the unique streamwisely-decaying manners of the maximum turbulence-intensity  $(u_{rms})_{max}$ , as well as the maximum mean-velocity  $(u_{mean})_{max}$  in Subsection 3.2. To be conclude, this is independent of both  $l/h$  and  $Re$ .

To be specific, as mentioned in Subsection 3.2, all the streamwise decays of the maximum value  $(u_{mean})_{max}$  in the transverse mean-velocity profiles are close to the theory by Tollmien (quoted from Rajaratnam (1976)) at  $x/h = 10.0 - 100$ , being independent of  $l/h$  and  $Re$ . On the other hand, the maximum value  $(u_{rms})_{max}$  in the transverse turbulence-intensity profile grows in the streamwise direction at  $x/h \lesssim 10$ , and decays in the streamwise direction at  $x/h \gtrsim 10$ , for all the cases. Thus,  $(u_{rms})_{max}$  always attains a peak value at  $x/h \simeq 10$ . As well as  $(u_{mean})_{max}$ , all the streamwise decays of

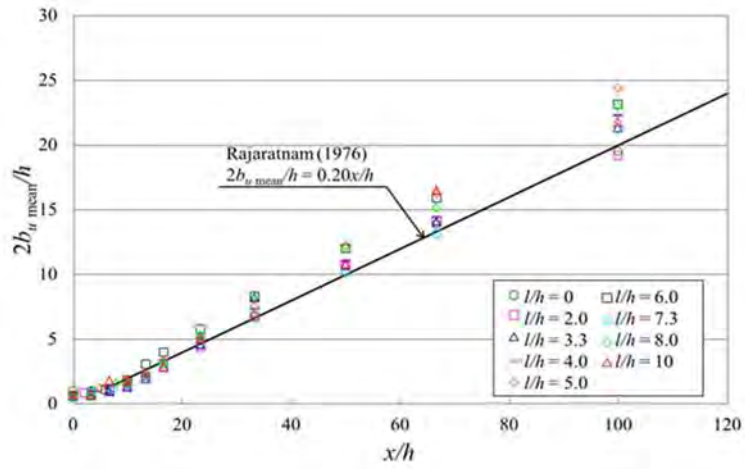


**Figure 6.** Streamwise distributions of the half width  $2b_{u \text{ mean}}$  of mean-velocity profile at midspan ( $y/h = 0$ ) for  $l/h = 0 - 10$  and  $Re = 1,000$ .

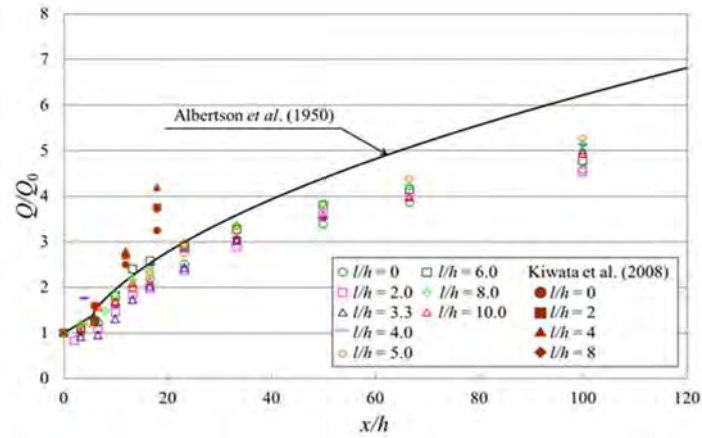


**Figure 7.** Streamwise distributions of time-mean local flow rate  $Q$  at midspan ( $y/h = 0$ ) for  $l/h = 0 - 10$ ,  $Re = 1,000$ .

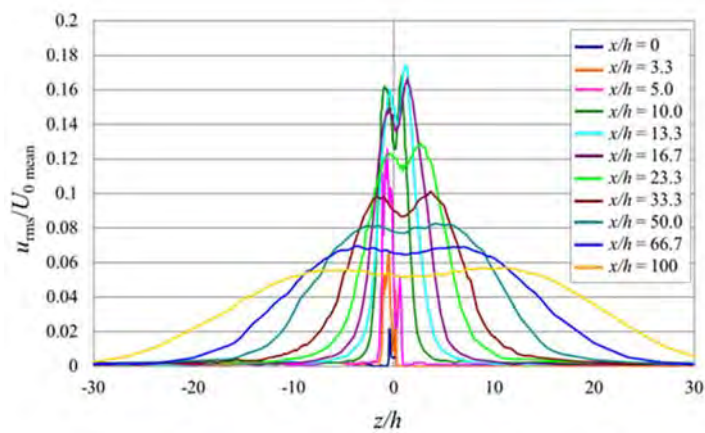


**Figure 8.** Turbulence-intensity profiles in the  $z$  direction at midspan ( $y/h = 0$ ) for  $l/h = 5.0$  and  $Re = 1,000$ .

$(u_{rms})_{max}$  are identical with one another, being independent of  $l/h$  and  $Re$ . The influence of  $l/h$  upon the peak value of  $(u_{rms})_{max}$  is not negligible but complicated. And, the influence of  $Re$  upon the peak value is rather monotonical; namely, the peak value tends to decrease with increasing  $Re$ . The peak value on the no-lip side tends to appear at smaller  $x/h$  than that on the lip side.

### 3.7. Streamwise Variation of Jet's Bias on Turbulence-Intensity

Figure 10 shows the streamwise distributions of a jet's bias  $(z_{u\ mean})_{max}$  on turbulence-intensity on the lip side, namely, a local turbulence-intensity-profile centre, for several values of  $l/h$ . We define  $(z_{u\ rms})_{max}$  as the value of  $z$  where the transverse turbulence-intensity profile attains the maximum  $(u_{rms})_{max}$  on the lip or no-lip side at each  $x$ , as shown in figure 8.

At first, when we consider the far downstream at  $x/h \geq 10$ , we can clearly confirm the streamwise growth of the jet bias suggested in figure 8. Concretely speaking, the jet bias for  $l/h = 0$  is slightly positive and is almost in proportion to  $x/h$ .

As well, the jet biases for  $l/h = 2.0$  and  $3.3$  show the above two features such as (1) the upward deflection and (2) the spatial linearity of the jet axis. However, from a quantitative viewpoint, we can find an effect of  $l/h$  upon the jet bias, if we compare the results for  $l/h = 0$ . Namely, by the  $l/h$  effect, the large  $l/h$  becomes, the less upward the jet deflection is.

In contrast with the jet biases for  $l/h = 0, 2.0$  and  $3.3$ , the jet's biases for  $l/h = 4.0$  and  $5.0$  indicate the above two features. However, from a quantitative viewpoint, we can find an effect of  $l/h$  upon the jet bias, if we compare the results for  $l/h = 0$ . Namely, by the  $l/h$  effect, the large  $l/h$  becomes, the much more upward the jet deflection is.

Again, the jet biases for  $l/h = 6.0$  and  $8.0$  shown the above two features for  $l/h = 0$ . From a quantitative viewpoint, we can find an effect of  $l/h$  upon the jet bias. Namely, the jet's biases for  $l/h = 6.0$  and  $8.0$  almost coincide with that for  $l/h = 0$ .

As well, the jet's bias for  $l/h = 10$  shows the above two features for  $l/h = 0$ . However, from a quantitative viewpoint, we can find a  $l/h$  effect upon the jet's bias. Namely, the jet's bias for  $l/h = 10$  almost coincide with those for  $l/h = 2.0$  and  $3.3$ .

### 3.8. Streamwise Growths of Half Width on Turbulence-Intensity and of Turbulence-Energy Integral

Figure 11 shows the streamwise distributions of the half width  $2b_{u\ rms}$  of turbulence-intensity profile at midspan ( $y/h = 0$ ) for several values of  $l/h$ . Both the axes are normalised by  $h$ . For reference, the figure also shows the theory by Rajaratnam (1976) [9] such as Eq. (1).

We can see that a linearly increasing manner of the half width  $2b_{u\ rms}$ . More specifically, at  $x/h \lesssim 10$ ,  $2b_{u\ rms}/h$  is almost unity, being independent of  $l/h$ . This is consistent with the existence of the potential core. At  $x/h \gtrsim 10$ ,  $2b_{u\ rms}/h$  increases linearly with increasing  $x/h$ . Moreover, we can see that all the results almost collapse on an empirical formula, being independent of  $l/h$ . The formula is given by

$$2b_{u\ rms} = 7/4(0.20x). \quad (3)$$

All the results are always larger than the Rajaratnam's theory, as well as those for  $Re = 6,000$ .

Figure 12 shows the streamwise distributions of a cross-streamwise integral  $I_{sq(u\ rms)}$  of turbulence energy at midspan ( $y/h=0$ ) for  $l/h = 0 - 10$ . Turbulence-energy integral  $I_{sq(u\ rms)}$  tends to be independent of  $l/h$  in such a far downstream as  $x/h \gtrsim 10$ . In the far downstream,  $I_{sq(u\ rms)}$  becomes small with decreasing  $Re$ . In such a near downstream as  $x/h \lesssim 10$ ,  $I_{sq(u\ rms)}$  rapidly increases from zero, and approaches to a constant value of about 100. To be exact, there exist the fluctuation of  $I_{sq(u\ rms)}$  in the downstream at  $x/h \lesssim 10 - 100$ , for  $l/h = 5.0 - 8.0$ .

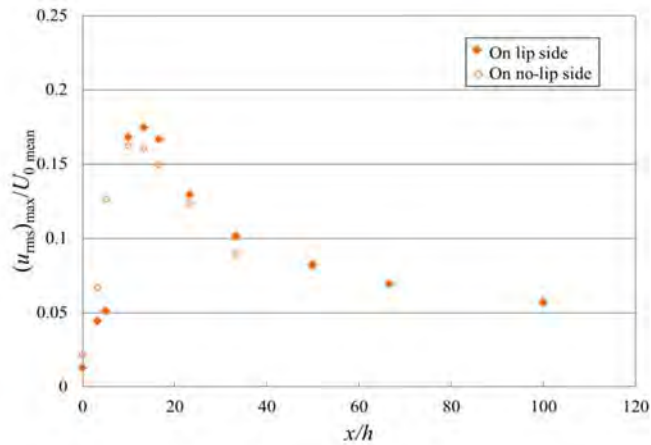


**Figure 9.** Streamwise distributions of the maximum turbulence-intensity at midspan ( $y/h = 0$ ) for  $l/h = 5.0$  and  $Re = 1,000$ .

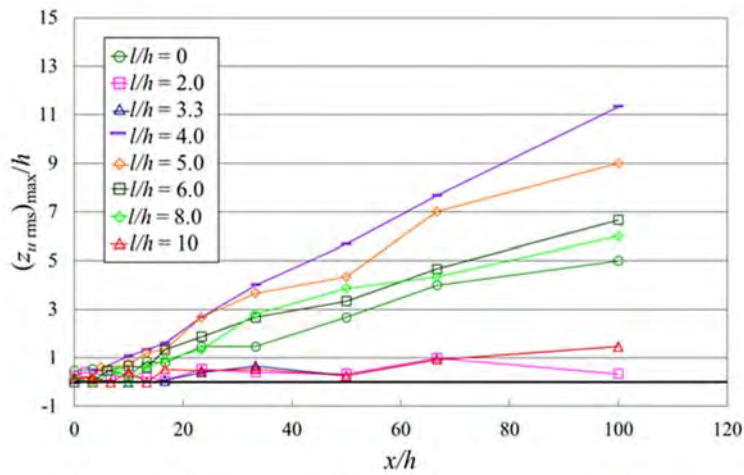


**Figure 10.** Streamwise distributions of jet-turbulence-peak bias  $(z_{u\text{ rms}})_{\text{max}}$  at midspan ( $y/h = 0$ ) on lip side for  $l/h = 0 - 10$  and  $Re = 1,000$ , on lip side ( $z/h > 0$ ).

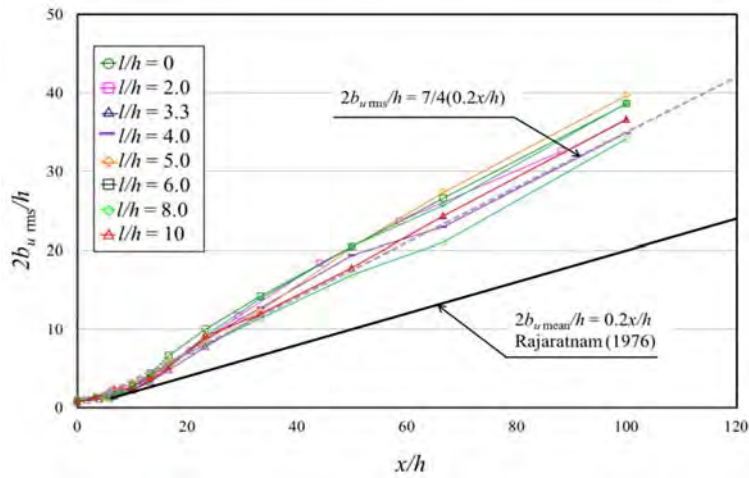


**Figure 11.** Streamwise distributions of the half width  $2b_{u,rms}$  of turbulence-intensity profile at midspan ( $y/h = 0$ ) for  $l/h = 0 - 10$  and  $Re = 1,000$ .

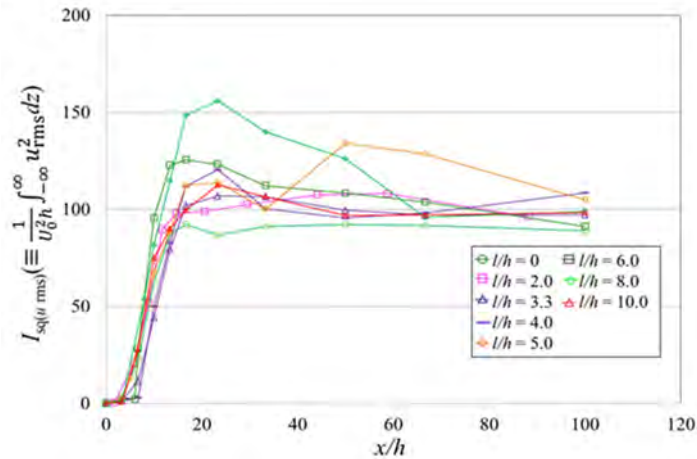


**Figure 12.** Streamwise distributions of a cross-streamwise integral  $I_{sq(u,rms)}$  of turbulence energy at midspan ( $y/h=0$ ) for  $l/h = 0 - 10$  and  $Re = 1,000$ .

#### 4. Summary

We have achieved such a sufficiently-two-dimensional jet as the quasi-plane jet by Mi *et al.* (2005), at  $x/h < 100$  for the reduced lip length  $l/h = 0 - 10.0$  and  $Re = 1,000$ . Referring to Hirata et al. (2010) where experiments are conducted at  $l/h = 0 - 5.0$  and  $Re = 6,000$ , we have obtained the following conclusions.

The main features about such four quantities concerning mean-velocity profile as  $(u_{\text{mean}})_{\text{max}}$ ,  $(z_{u_{\text{mean}}})_{\text{max}}$ ,  $2b_{u_{\text{mean}}}$  and  $Q$  at  $Re = 1,000$  are similar with those at  $Re = 6,000$ . However to be strict, we can observe small influences of  $Re$  upon three of all the four quantities, namely,  $(u_{\text{mean}})_{\text{max}}$ ,  $(z_{u_{\text{mean}}})_{\text{max}}$  and  $Q$ . On the other hand, we can approximately ignore the  $Re$  influence upon  $2b_{u_{\text{mean}}}$ . The two small  $Re$  influences upon  $(u_{\text{mean}})_{\text{max}}$  and  $Q$  are consistent, because of the enhanced viscous effect with decreasing  $Re$ . On the other hand, it seems difficult to coherently explain the  $Re$  influence upon  $(z_{u_{\text{mean}}})_{\text{max}}$  at the present stage. Such four quantities concerning turbulence-intensity profile as  $(u_{\text{rms}})_{\text{max}}$ ,  $(z_{u_{\text{rms}}})_{\text{max}}$ ,  $2b_{u_{\text{rms}}}$  and  $I_{\text{sq}(u_{\text{rms}})})$  well correspond with mean-velocity profile.

Specifically speaking, at  $x/h \gtrsim 10$ , the jet is regarded to fully develop being independent of both  $l/h$  and  $Re$ , on the basis of (1) the similar profiles of mean-velocity and turbulence-intensity, (2) the unique streamwisely-decaying manners of the maximum mean-velocity  $(u_{\text{mean}})_{\text{max}}$  and the maximum turbulence-intensity  $(u_{\text{rms}})_{\text{max}}$ , (3) linearly-increasing manners of jet's bases  $(z_{u_{\text{mean}}})_{\text{max}}$  and  $(z_{u_{\text{rms}}})_{\text{max}}$  in the streamwise direction, (4) linearly-increasing manners of half widths  $2b_{u_{\text{mean}}}$  and  $2b_{u_{\text{rms}}}$ , (5) flow rate  $Q$  and turbulence-energy integral  $I_{\text{sq}(u_{\text{rms}})})$ . At  $x/h \gtrsim 10$ , the influences of  $l/h$  is remarkable only upon jet's biases like  $(z_{u_{\text{mean}}})_{\text{max}}$  and  $(z_{u_{\text{rms}}})_{\text{max}}$ , and not upon the maximum values, like  $(u_{\text{mean}})_{\text{max}}$  and  $(u_{\text{rms}})_{\text{max}}$ , jet's widths like  $2b_{u_{\text{mean}}}$  and  $2b_{u_{\text{rms}}}$ . Flow rate  $Q$  is independent of  $l/h$  in both near (at  $x/h = 0 - 10.0$ ) and far downstreams (at  $x/h = 10.0 - 100$ ), but depends upon  $Re$ ; namely,  $Q$  for  $Re = 1,000$  is smaller at each  $x/h$  than those for  $Re = 6,000$  which almost coincide with Albertson et al. (1950). Turbulence-energy integral  $I_{\text{sq}(u_{\text{rms}})})$  tends to be independent of  $l/h$  in such a far downstream as  $x/h \gtrsim 10$ .

According to Hirata et al. (2010), an asymmetrical two-dimensional nozzle has potential for smart jet's control especially for jet's deflection at high  $Re$ . the present study has revealed that this potential is effective even at low  $Re$  with slight modifications.

#### References

- [1] Hirata, K., Funaki, J., Kubo, T., Hatanaka, Y., Matsushita, M. and Shobu, K. 2009 *J. Fluid Science & Technology, JSME*, **Vol. 4**, No. 3, pp. 578 – 588.
- [2] Funaki, J., Kobayashi, D., Shobu, K. and Hirata, K. 2009 *J. Fluid Science & Technology, JSME*, **Vol. 4**, No. 3, pp. 673 – 686.
- [3] Förthmann, E. 1936 *NACA Technical Memorandum*, No. 789, pp. 1 – 18.
- [4] Goertler, H. 1942 *Zeitschrift für Angewandte Mathematik und Mechanik*, **Vol. 22**, No. 5, pp. 244 – 254.
- [5] Van der Hegge Zijnen, B. G. 1958 *Applied Scientific Research, Section A*, **Vol. 7**, pp. 256 – 276.
- [6] Quinn, W. R. 1992 *Experimental Thermal and Fluid Science*, **Vol. 5**, pp. 203 – 215.
- [7] Mi, J., Deo, R. C. and Nathan, G. J. 2005 *Physics of Fluids*, **Vol. 17**, No. 6, pp. 068102.1 – 068102.4.
- [8] Deo, R.C. 2005 *PhD Thesis*, Adelaide Univ.
- [9] Horne, C., Jonkouski, G. and Karamcheti, K. 1981 *AIAA 7th Aeroacoustics Conference*, pp. 1 – 11.
- [10] Husain, Z. D. and Hussain, A. K. M. F. 1983 *AIAA Journal*, **Vol. 21**, No. 11, pp. 1512 – 1517.
- [11] Kiwata, T., Kimura, S., Komatsu, N., Murata H. and Kim, Y. H. 2009 *J. Fluid Science & Technology, JSME* **Vol. 4**, No. 2, pp. 268 – 278.
- [12] Hirata, K., Shobu, K., Murayama, T. and Funaki, T. 2010 *J. Fluid Science & Technology, JSME*, **Vol. 5**, No. 1, pp. 183 – 199.
- [13] Rajaratnam, N. 1976 *Turbulent Jets*, Elsevier, Amsterdam.